International Journal of Academic and Applied Research (IJAAR)
ISSN: 2643-9603
Vol. 4 Issue 2, February – 2020, Pages: 41-50

Green Synthesis of Gold Nanoparticles Using Lallamantia Royleana Seed Extract and Evaluation of Its Antioxidant Activity

Samina Rashid Ahmed, Sadia Noor, Maria Anwar Khan*
Department of chemistry, Lahore College for Women University, Lahore, Pakistan
*Doc.mariakhan@gmail.com

Abstract**:** *The development of an eco-friendly protocol for the synthesis of nanomaterials is an important aspect of research in nanotechnology. The present study demonstrates a facile and rapid synthesis of gold nanoparticles (AuNPs) by Lallementia royleana (LR) seed extract for some potential biomedical applications. The synthesized AuNPs were characterized by UV-visible spectroscopy, Fourier transform infrared (FTIR) spectroscopy, atomic absorption spectroscopy (AAS) and thermogravimetric analysis (TGA). The LR seed extract played a dual role by reducing Au^{+3} to Au^{0} and stabilizing the resulting NPs. The formation of AuNPs was confirmed through UV-visible spectroscopy by measuring characteristic λ_{SPR} peaks between 532-554 nm. The different reaction parameters; amount of LR mucilage, temperature and pH were optimized using conventional method. The optimum conditions were found to be; LR amount (10.0 mL), temperature (60 ℃) and pH (12) to obtain the high yield of AuNPs with narrow size distribution. Fourier transform infrared analysis showed the interaction between AuNPs and functional groups responsible for reduction and stabilization. Unreacted amount of gold ions was measured by atomic absorption spectroscopy and maximum yield was found to be 94.45 %. The surface topography was observed by atomic force microscopy. The antioxidant potential of synthesized AuNPs was evaluated by DPPH, hydroxyl radical scavenging and reducing power assays which shows a concentration dependent effect on the antioxidant potential of AuNPs.*

Keywords—Green synthesis, *Lallementia royleana* seed extract, Gold nanoparticles, Thermogravimetric analysis, Antioxidant potential.

1. INTRODUCTION

Nanotechnology is an immensely developing field due to its extensive range of applications in different areas of technology and science. Nanoparticles (NPs), the fundamental building blocks of nanotechnology are of great worth owing to their potential applications in various areas, such as catalysis, photonic, health care, tissue engineering, drug delivery, molecular imaging [1], sensors, food industry and environmental, in fact in every field many more to count on [2]. Recent progresses of nanomaterials in several fields arise from their unique chemical and biological properties associated with nano − size, shape, composition and crystallinity [3, 4].

Among the metal nanoparticles, AuNPs being inert and relatively least cytotoxic are extensively used for biomedical catalysis [5]. The synthesis of AuNPs using various biological materials such as bacteria, fungi, yeast and plant extracts [6] has received a great deal of attention because of the availability of significant bioactive compounds and simple, eco-friendly and size-controlling approaches [7]. Recently Kotcherlakota *et al*. demonstrated the synthesis of highly biocompatible gold nanoparticles using *Zinnia elegans* plant leading to in vivo study of Near-Infrared Fluorescence (NIR)-based bio-imaging and cell labeling applications [8].

The rapid bio-reduction of chloroauric acid by *Chloroxylon swietenia* DC leaf extract to form well dispersed *C. swietenia* gold nanoparticles was studied by Balasubramani and the coworkers [9]. Yuan *et al*. reported a rapid biosynthesis method for AuNPs from *Capsicum annuum* var. *grossum* pulp extract in a single-pot process [10]. Recently a green approach for the synthesis of gold nanoparticles using *Eupatorium odoratum* leaf extract [11], *Annona muricata* leaf extract [12], aqueous extract from *Crinum latifolium* leaves [13] and cinnamon (natural spice) [14] has been reported. Irfan *et al*. reported that ionic liquid mediated *Elaeis. guineensis* (oil palm) leaves extract can be used for reduction of gold precursor to obtain stable AuNPs [15]. Hoshyar *et al*. used crocin to fabricate AuNPs and studied their anti-cancer activities [16]. Barrios-Gumiel *et al*. reported heterofunctionalized gold nanoparticles with cationic carbosilane dendrons (first to third generations, 1-3G) and (polyethylene) glycol (PEG) ligands in the presence of a reducing agent [17].

Hence, in the present study we demonstrated the use of *Lallementia royleana* seed extract mediated green synthesis of gold nanoparticles having exceptionally high antioxidant potential.

2. MATERIALS AND METHODS

2.1 Chemicals

Chloroauric acid ($HAuCl_4.3H_2O$), hydrochloric acid (HCl), sodium hydroxide (NaOH), 2,2-diphenyl-1-picrylhydrazyl (DPPH), ascorbic acid (AA), dimethyl sulfoxide (DMSO), potassium ferrocyanide ($K_4[Fe(CN)_6].3H_2O$), trichloroacetic acid (TCA), ferric chloride ($FeCl_3$), potassium dihydrogen phosphate (KH_2PO_4), salicylic acid (SA), ferrous sulphate ($FeSO_4.7H_2O$), hydrogen peroxide (H_2O_2) and other chemicals were of analytical grade and procured from Sigma Aldrich Co.,

USA. All chemicals were used as received without any further purification. *LR* seeds were obtained from local market. Double distilled water (DDW) was used in this work.

2.2 Isolation and purification of mucilage from LR seeds

Dried seeds (5.0 g) of LR were soaked in DDW (400 mL) for 2 h in a clean environment. Gelatinous layer formed around seeds, was then homogenized in kitchen blender for 1-2 min. The clear gelatinous material was isolated from seeds by centrifugation at 4000 rpm for 40 min. The LR gel was filtered under vacuum filtration using muslin cloth and washed several times with DDW. The isolated LR gel was stored in fridge to prevent the fungal growth and then used for further characterization.

2.3 Synthesis of LR-AuNPs

$HAuCl_4.3H_2O$ solution (1.0 mM) was taken (10.0 mL) in a round bottom flask into which varying amounts of purified *LR* gel (2.0-10.0 mL) were added in drop wise manner and total volume of the mixture was made up to 20.0 mL using DDW under constant stirring at 25 ˚C. A change in colour from yellow to purple was observed after 20-30 min which confirms the formation of *LR*-AuNPs. The UV-visible spectra of synthesized AuNPs were recorded in 200-800 nm range using UV-visible spectrophotometer.

2.4 Optimization of reaction parameters

The reaction parameters (pH, temperature and amount of *LR* mucilage) were optimized to get control over the yield, size and concentration of NPs by changing one parameter at a time and keeping rest of the parameters constant. In various experiments, the pH of the reaction mixture was maintained with the help of HCl (0.1 M) or NaOH (0.1 M) solutions. The different reaction parameters were determined from *LR* gel amount, temperature (25 ˚C and 60 ˚C), pH (4, 8 and 12) and time respectively.

2.5 Characterization

2.5.1 UV-visible spectroscopy and FTIR analysis

The UV-visible spectra of the synthesized AuNPs were recorded in 300-800 nm range using UV/Vis Spectrophotometer (U-2800 Hitachi, Japan) to observe the characteristic λ_{SPR} of AuNPs. Functional group analysis of *LR* extract and synthesized AuNPs was carried out using (IRTracer-100, Shimadzu), in the range of 4000-400 cm^{-1}.

2.5.2 Atomic absorption spectroscopy and Thermal analysis

A polarized Zeeman atomic absorption Z-5000 spectrophotometer (Hitachi, Japan) equipped with single element hollow cathode lamp (6.0 mA for gold) and 10 cm of burner head and air acetylene burner was used for the determination of gold. The wavelength at 242.8 nm (resonance line), the spectral band width at 0.5 nm and the ratio of air-acetylene at 4.7 were set. Thermogravimetric analysis of the *LR* gel and synthesized *LR*-AuNPs was performed at a temperature range of 20 ˚C-700 ˚C using SDT (Q600-TA Instruments, USA) in a dry air atmosphere.

2.5.3 Atomic force microscopy

To study the surface morphology and distribution pattern, AFM analysis of *LR*-AuNPs was carried out using scanning probe microscope (SPM-9500 J3, Shimadzu, Japan) under normal atmospheric conditions. For this analysis, a freshly prepared sample was deposited on a fine metal surface in dust-free environment.

2.6 In vitro antioxidant studies

2.6.1 DPPH free radical scavenging assay

DPPH is a stable, purple coloured free radical which turns yellow when scavenged. This property of the radical was exploited to show the free radical scavenging activity of the synthesized *LR*-AuNPs. DPPH solution (0.1 mM) in DMSO was prepared and mixed (2.0 mL) vigorously with different concentrations (12.5-200 µL/mL in DMSO) of gold solution. At room temperature the reaction mixture was incubated in the dark for 30 minutes. After incubation, the absorbance (A) measurements was made at 517 nm. The procedure was repeated for control solution of (*LR*). Ascorbic acid (AA) was taken as reference (R). The percentage inhibition of the radicals by AuNPs was determined using the equation:

$$\% \text{ Inhibition} = A_{blank} - A_{sample} / A_{sample} \times 100 \quad (1)$$

2.6.2 Reducing power assay

In this assay, various concentrations (12.5-200 µL/mL) of AuNPs and *LR* were separately mixed (1.0 mL) with PBS (0.2 M, pH 6.6) and potassium ferrocyanide (1.0 mL; 1%) and then incubated for 20 min. at 50 ˚C. After that TCA (1.0 mL; 10 %) was added and then centrifuged at 3000 rpm for 10 min. To supernatant (1.0 mL), of DDW was added (1.0 mL) followed by of $FeCl_3$ (0.5 mL; 0.01 %) and the absorbance was measured at 700 nm against PBS as blank. AA was used as positive control in this test. The percentage inhibition was determined using the equation:

$$\% \text{ Inhibition} = (A_{sample} - A_{negative\ control}) / (A_{positive\ control} - A_{negative\ control}) \times 100 \quad (2)$$

2.6.3 Hydroxyl radical scavenging assay

To different concentrations of AuNPs (12.5-200 µL/mL) and *LR* extract, salicylic acid (9.0 mM; 1.0 mL), $FeSO_4.7H_2O$ (9.0 mM; 1.0 mL) and H_2O_2 (1.0 mL) were added. The reaction mixture was incubated at 37 ˚C for 60 minutes. After incubation the absorbance was measured at 510 nm using a UV-visible spectrophotometer. Negative control was prepared without samples, whereas AA was taken as positive

International Journal of Academic and Applied Research (IJAAR)
ISSN: 2643-9603
Vol. 4 Issue 2, February – 2020, Pages: 41-50

control. The percentage of hydroxyl radical scavenging activity for test samples was determined using this equation,

$$\% \text{ Inhibition} = (A_{sample} - A_{negative\ control}) / (A_{positive\ control} - A_{negative\ control}) \times 100 \quad (3)$$

3. RESULTS AND DISCUSSION

3.1 Isolation and purification of mucilage from *LR* seeds

LR seed is a natural polysaccharide consisting of dietary fiber, crude ash, fats, protein and crude oil respectively [18]. When the seed has been soaked in water, it absorbs water and a mucilaginous layer of polysaccharide is formed, that surrounds it. This mucilage content has interesting properties for pharmaceutical industries and in the present study; it has played dual role as a stabilizing and reducing agent respectively.

3.2 Synthesis of *LR*-AuNPs

LR-AuNPs were synthesized using *LR* seed mucilage which acted as both the reducing and stabilizing agent and $HAuCl_4.3H_2O$ as gold precursor. The reduction of Au^{3+} ions to Au^0 was indicated by colour change from pale yellow to pinkish violet, when seed mucilage was mixed with $HAuCl_4.3H_2O$ as depicted in Fig. 1. The UV-visible spectra were recorded in 200-800 nm range to observe the characteristic absorption bands of AuNPs.

Fig. 1: *Change in color from yellow to pinkish violet confirming the formation of Lallemantia royleana-Gold nanoparticles (LR-AuNPs)*

3.3 Optimization of reaction conditions

Reaction conditions such as temperature, pH and amount of *LR* seed mucilage play a vital role in the synthesis of *LR*-AuNPs. Optimization of reaction parameters was achieved conventionally by varying amount of mucilage, temperature and keeping the amount of $HAuCl_4.3H_2O$ (10.0 mL) constant. UV-visible spectroscopy was used to study the effect of all these parameters over synthesis rate. The obtained results confirmed that by increasing concentration of mucilage (10.0 mL) and temperature (60 ˚C) at pH 12, absorbance increases and wavelength (λ_{SPR}) was shifted towards shorter wavelength resulting decrease in the size of AuNPs as shown in Fig. 2 (A and B).

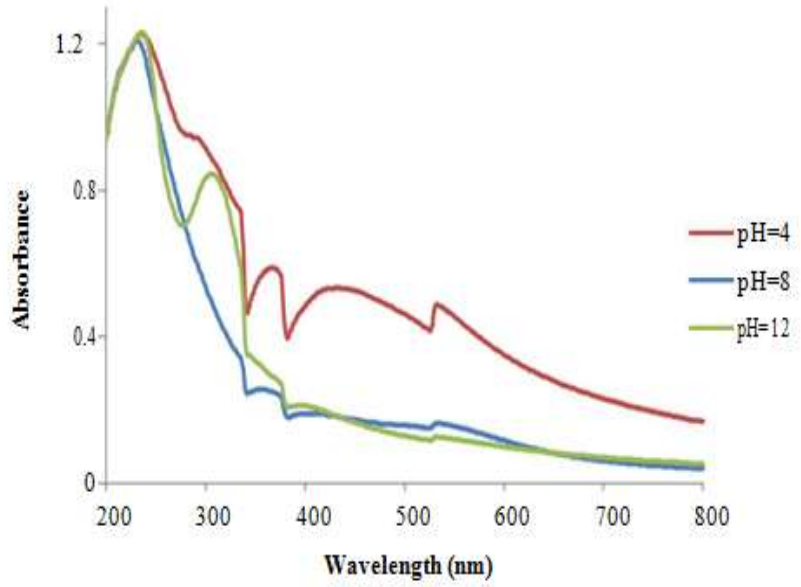

(A)

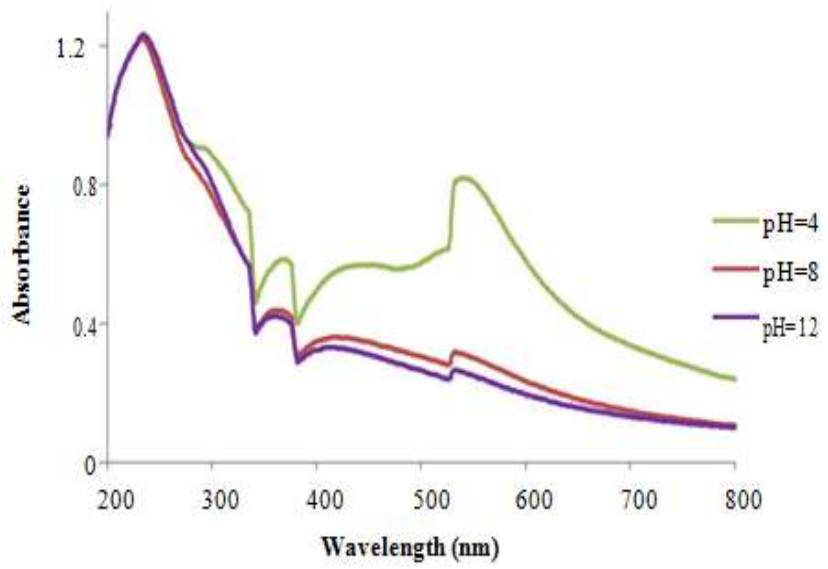

(B)

Fig. 2: *UV-visible spectra of LR-AuNPs by varying the amount of LR mucilage and pH at (A) 25 ˚C; (B) 60 ˚C*

3.4 Characterization of *LR*-AuNPs

3.4.1 UV-visible spectroscopy and FTIR spectroscopy

Synthesis of *LR*-AuNPs was monitored by recording UV-visible spectra between 300-800 nm. The maximum value for λ_{SPR} was 546 nm, which is a characteristic of spherical shaped AuNPs recorded at 60 ˚C. By increasing the amount of mucilage, increased absorbance was observed with decreasing wavelength indicating the formation of small sized AuNPs as shown in Fig. 3.

The FTIR analysis showed the characteristic absorption bands, which revealed the presence of O−H group (~ 3387.00086 cm^{-1}), N−H group (~ 3271.0996 cm^{-1}), C−H group (2920.227424 cm^{-1}) and C−O−C linkage (1029.98977 cm^{-1}) in the *LR* mucilage as shown in Fig. 4 (A). The FTIR spectrum of *LR*-AuNPs showed bands shifted for O−H group (2918.318 cm^{-1}), N−H group (3295.8595 cm^{-1}), C−H group (670.779 cm^{-1}) and C−O−C linkage (1145.424 cm^{-1}) respectively as shown in Fig. 4 (B).

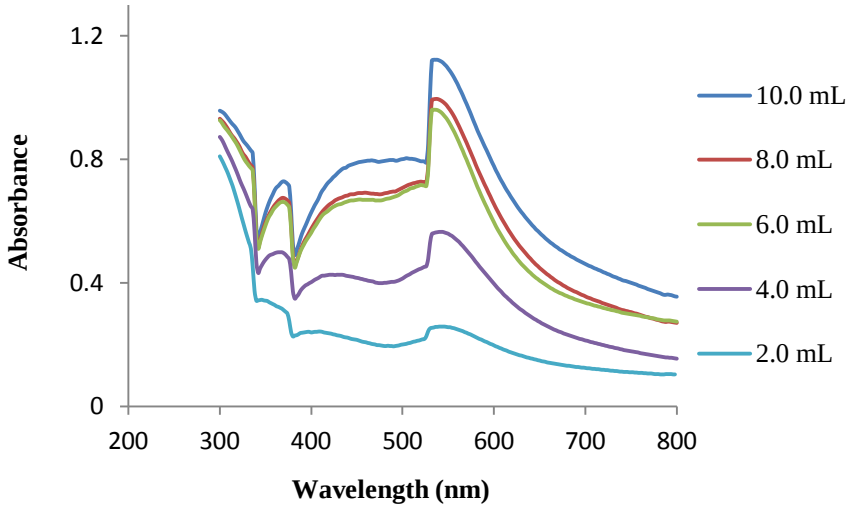

Fig. 3*: UV-visible spectra of LR-AuNPs with varying amount of LR mucilage at 60 ˚C*

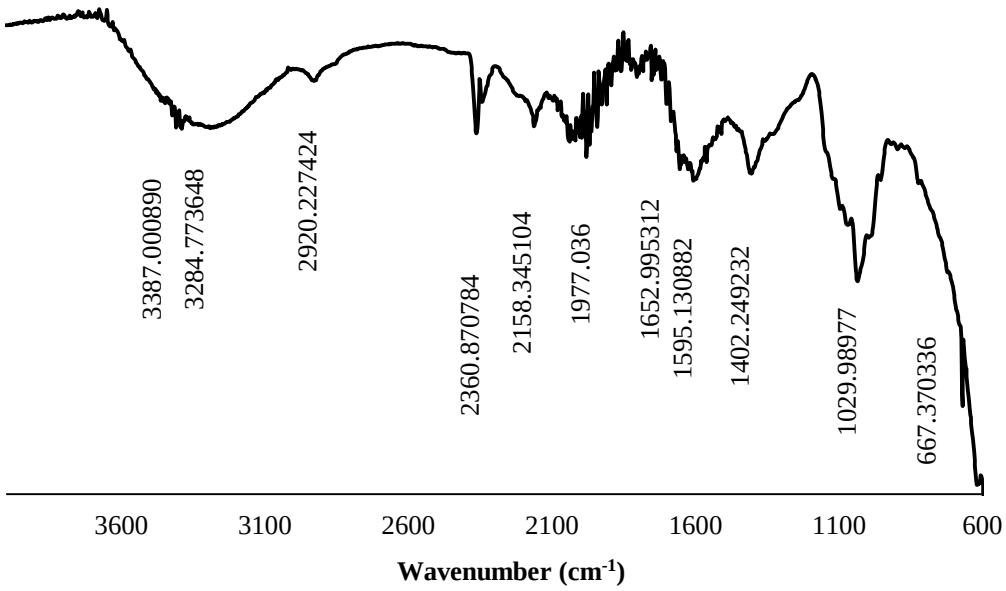

(A)

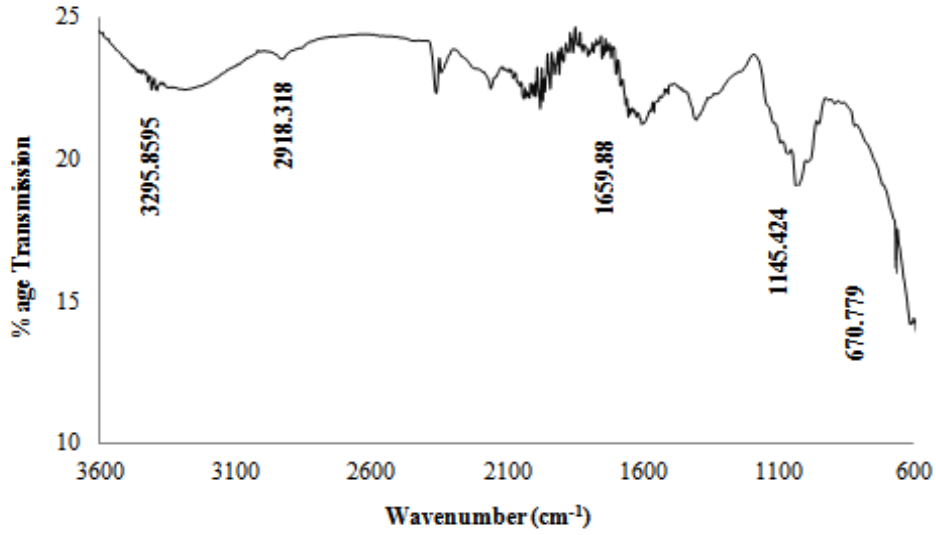

(B)

Fig. 4: *Fourier-transform infrared spectroscopy (FTIR) spectrum of (A) Lallemantia royleana (LR) mucilage (B) Lallemantia royleana (LR) mucilage with Gold nanoparticles (AuNPs)*

3.4.2 Atomic absorption spectroscopy and Thermal analysis

AAS has been used to determine the varying concentration of Au^{+} ions in the solution after synthesis. Results showed that the concentrations of Au-ions reduced, due to conversion of Au^{+} to Au^{0}. The graph was plotted between concentrations (ppm) of AuNPs and absorbance, which gave a straight line as shown in Fig. 5 (A) and (B) respectively. The straight-line equation was used to calculate the concentration of AuNPs which is given in Table. 1.

The involvement of various secondary metabolites from *LR* gel in the synthesis of *LR*-AuNPs and their thermal behavior were further characterized by the TGA analysis at a range of 20-700 ˚C as shown in Fig. 6. The results showed a three-stage weight loss of 24.73 %, indicating that at higher temperature, the organic compounds from *LR* gel surrounding the *LR*-AuNPs, which acted as the capping agent for AuNPs, were completely degraded. Absorbed water was evaporated at the first stage (20-178 ˚C). At the second stage (178-386 ˚C), most of the organic compounds were removed by combustion. At the third stage (387-700 ˚C), the weight changes were minimized, and the little weight loss observed was likely related to removal of large polymers [19].

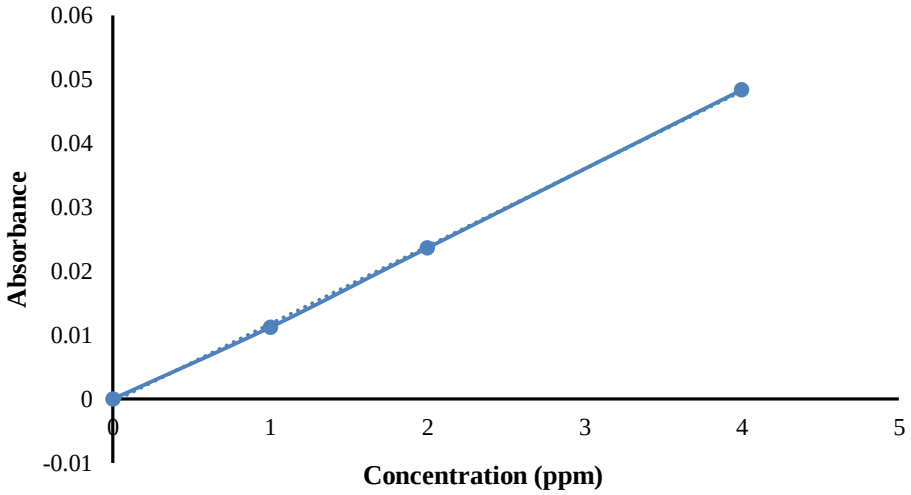

Fig. 5: *(A) Linear relationship between absorbance and concentration of Gold nanoparticles (AuNPs) [PPM]*

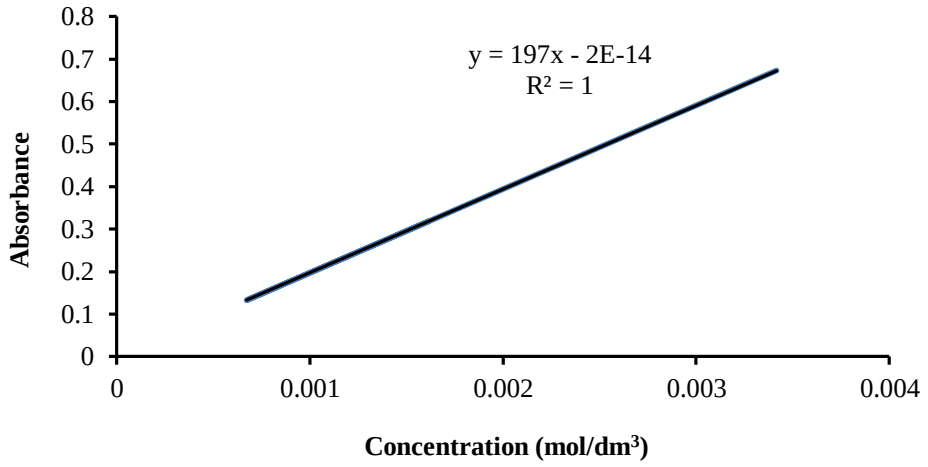

Fig. 5: *(B) Absorbance variation with concentration of unreactive Gold nanoparticles (AuNPs) [mol/dm^3]*

Table 1: Concentration and % age yield of AuNPs determined by varying amount of *LR* mucilage

Amount of LR-Extract (mL)	*$HAuCl_4$ (mL)*	*H_2O (mL)*	*Absorbance (Abs)*	*Conc. Of Au^+ ions (unreacted) (x) Ppm*	*Conc. of AuNPs (ppm) (reacted)*	*Conc. of AuNPs (mol/dm^3)*	*Percentage Yield (%)*
10	10	0	0.3183	26.34	170.65	0.00086	86.62
8	10	2	0.2352	19.47	177.53	0.000901	90.11
6	10	4	0.1326	11	186	0.0009441	94.45
4	10	6	0.3004	24.86	172.13	0.00087	87.36
2	10	8	0.6729	55.65	141.34	0.000717	71.74

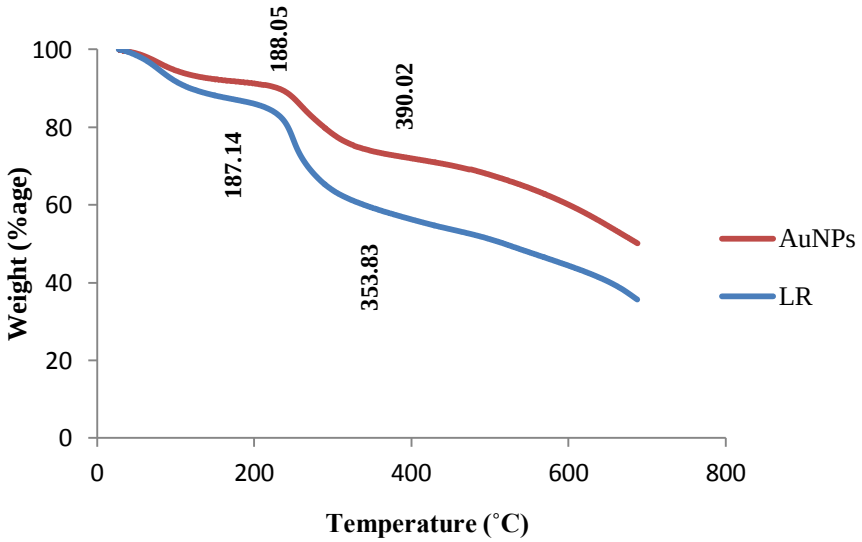

Fig. 6: *Thermogravimetric analysis (TGA) analysis of Gold nanoparticles (AuNPs) and Lallemantia royleana (LR) extract*

3.4.3 Atomic force microscopy

For this analysis, a freshly prepared sample was deposited on a fine copper metal surface in dust-free environment. Surface morphologies of *LR*-AuNPs have been depicted in the AFM image (Fig. 7). The roughness of the surface is due to dispersion of the AuNPs in polymeric matrix [20].

Fig. 7: *Atomic force microscopy (AFM) image of Lallemantia royleana- Gold nanoparticles (LR-AuNPs)*

3.5 Evaluation of antioxidant activity of *LR*-AuNPs

Several *in vitro* assays have been used to screen plants for their antioxidant potential and in most of these assays they revealed potent antioxidant activity. The free radical quenching ability of *LR* and *LR*-AuNPs was assessed by different *in vitro* assays.

3.5.1 DPPH assay

In the present study, the *LR* and *LR*-AuNPs have exhibited a higher potential in scavenging DPPH as shown in Fig. 8 (A). The scavenging action increases with increased concentration of the *LR* and *LR*-AuNPs and has been found to be comparable to that of AA. Both *LR* and *LR*-AuNPs have showed maximum percentage inhibition at concentration of (200 µL/mL) against AA as standard. The antioxidant activity of formulated *LR*-AuNPs was profoundly higher due to the presence of monosaccharides as reducing and stabilizing agents [21].

3.5.2 Reducing power assay

The reduction ability of *LR* and *LR*-AuNPs has shown dose-dependent reducing power. *LR*-AuNPs have less scavenging activity as compared to the *LR* because the pure plant extract is a rich source of reducing sugars which shows maximum activity. The reducing power activity of *LR* and *LR*-AuNPs increases with increasing concentration (200 µL/mL) as shown in Fig. 8 (B). It depicted the role of reducing sugars in reduction and functionalization of biocompatible *LR*-AuNPs [22].

3.5.3 Hydroxyl radical scavenging assay

Hydroxyl radical scavenging effect of *LR* and *LR*-AuNPs has been investigated and the results were revealed as relative activity against the standard AA. The results showed that both *LR* and *LR*-AuNPs were potent in scavenging the hydroxyl radicals at (200 µL/mL) concentration as shown in Fig. 8 (C). It has been reported that AuNPs possess unique morphology; high surface area to volume ratio which can easily accept electrons from (•OH) radical and plays a vital role in scavenging these free radical [22].

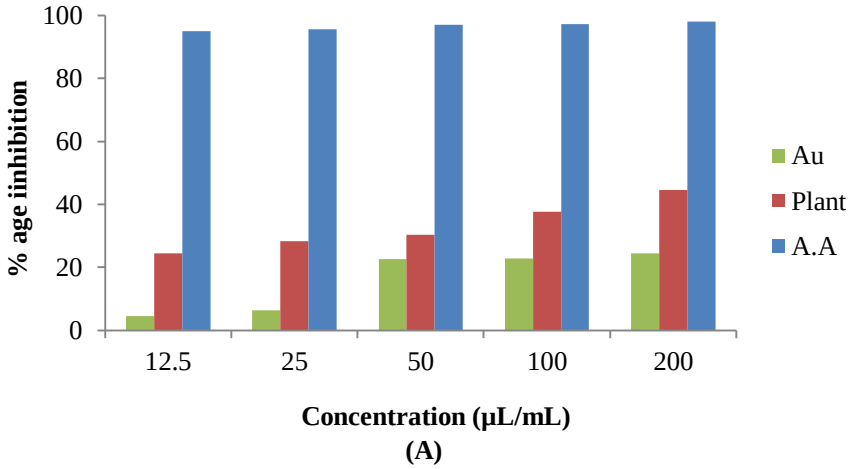

(A)

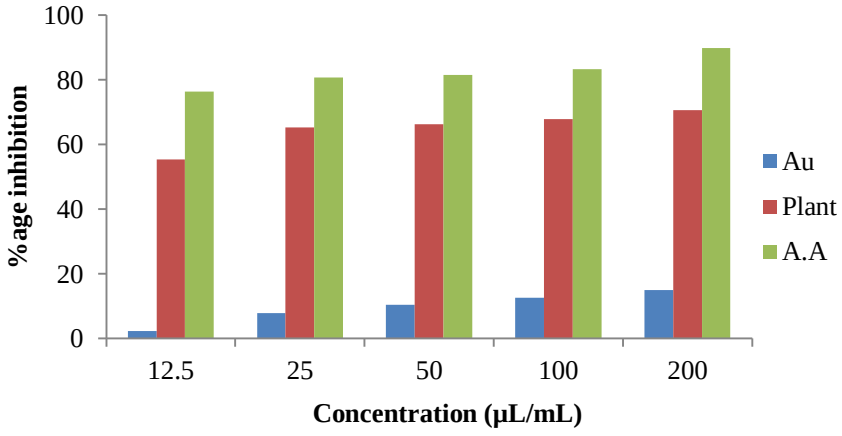

(B)

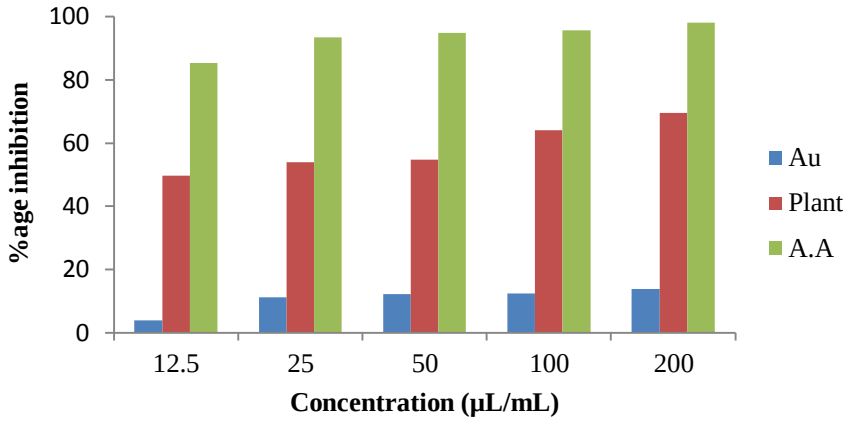

(C)

Fig. 5*: In vitro antioxidant activity (A) DPPH assay; (B) Reducing power assay; (C) Hydroxyl radical scavenging assay express the antioxidant capacity of formulated LR-AuNPs*

CONCLUSION

Green synthesis of NPs has been proved to be one of the flourishing fields. The present work provides a simple, fast, non-toxic, eco-friendly and an effective way to fabricate AuNPs using *Lallementia royleana* seed extract which played a dual role as capping and stabilizing agent. The antioxidant potential has been evidenced through various *in vitro* assays such as DPPH, reducing power and hydroxyl radical scavenging assays respectively. The outcome of this study emphasized that the synthesized *LR*-AuNPs possess excellent stability and biocompatibility and thus can be employed for wide spectrum of biomedical applications.

ACKNOWLEDGEMENT

The authors are thankful to Lahore College for Women University for facilitating this search.

CONFLICT OF INTEREST: Nil

REFERENCES

[1] Paul, B., Bhuyan, B., Purkayastha, D. D., & Dhar, S. S. (2016). Photocatalytic and antibacterial activities of gold and silver nanoparticles synthesized using biomass of *Parkia roxburghii* leaf, J. Photochem. Photobio. B: Biol., vol. 154, pp. 1-7.

[2] Macías-Martínez, B. I., Cortés-Hernández, D. A., Zugasti-Cruz, A., Cruz-Ortíz, B. R., & Múzquiz-Ramos, E. M. (2016). Heating ability and hemolysis test of magnetite nanoparticles obtained by a simple co-precipitation method, J. Appl. Res. Tech., vol. 14(4), pp. 239-244.

[3] Verma, A., & Mehata, M. S. (2016). Controllable synthesis of silver nanoparticles using Neem leaves and their antimicrobial activity, J. Rad. Res. Appl. Sci., vol. 9(1), pp. 109-115.

[4] Chanda, N., Kattumuri, V., Shukla, R., Zambre, A., Katti, K., Upendran, A., & Smith, C. J. (2010). Bombesin functionalized gold nanoparticles show in vitro and in vivo cancer receptor specificity, Proceed. Nat. Acad. Sci., vol. 107(19), pp. 8760-8765.

[5] Ahmad, A., Senapati, S., Khan, M. I., Kumar, R., Ramani, R., Srinivas, V., & Sastry, M. (2003). Intracellular synthesis of gold nanoparticles by a novel alkalotolerant actinomycete, *Rhodococcus* species. Nanotech., vol. 14(7), pp. 824-828.

[6] Cheong, S., Watt, J. D., & Tilley, R. D. (2010). Shape control of platinum and palladium nanoparticles for catalysis. Nanoscale, vol. 2(10), pp. 2045-2053.

[7] Gallina, M. E., Zhou, Y., Johnson, C. J., Harris-Birtill, D., Singh, M., Zhao, H., Ma, D., Cass, T., & Elson, D. S. (2016). Aptamer-conjugated, fluorescent gold nanorods as potential cancer theradiagnostic agents. Mat. Sci. Engineer.: C, vol. 59, pp. 324-332.

[8] Kotcherlakota, R., Nimushakavi, S., Roy, A., Yadavalli, H. C., Mukherjee, S., Haque, S., & Patra, C. R. (2019). Biosynthesized Gold Nanoparticles: In Vivo Study of Near-Infrared Fluorescence (NIR)-Based Bio-imaging and Cell Labeling Applications. ACS Biomat. Sci. Engineer., vol. 5(10), pp. 5439-5452.

[9] Balasubramani, G., Ramkumar, R., Krishnaveni, N., Sowmiya, R., Deepak, P., Arul, D., & Perumal, P. (2015). GC–MS analysis of bioactive components and synthesis of gold nanoparticle using *Chloroxylon swietenia* DC leaf extract and its larvicidal activity, J. Photochem. Photobio. B: Biol., vol. 148, pp. 1-8.

[10] Yuan, C. G., Huo, C., Yu, S., & Gui, B. (2017). Biosynthesis of gold nanoparticles using *Capsicum annuum var. grossum* pulp extract and its catalytic activity, Physica E: Low-dimen. Sys. Nanostruct., vol. 85, pp. 19-26.

[11] Roy, A., & Mohanta, B. (2019). Microwave-assisted green synthesis of Gold nanoparticles and its catalytic activity, Internat. J. Nano Dimension, vol. 10(4), pp. 359-367.

[12] Folorunso, A., Akintelu, S., Oyebamiji, A. K., Ajayi, S., Abiola, B., Abdusalam, I., & Morakinyo, A. (2019). Biosynthesis, characterization and antimicrobial activity of gold nanoparticles from leaf extracts of *Annona muricate*, J. Nanostruct. Chem., pp. 1-7.
[13] Vo, T. T., Nguyen, T. T. N., Huynh, T. T. T., Vo, T. T. T., Nguyen, T. T. N., Nguyen, D. T., & Nguyen, T. D. (2019). Biosynthesis of Silver and Gold Nanoparticles Using Aqueous Extract from *Crinum latifolium* Leaf and Their Applications Forward Antibacterial Effect and Wastewater Treatment, J. Nanomat., vol. 2019.
[14] Goyal, D., Saini, A., Saini, G. S. S., & Kumar, R. (2019). Green synthesis of anisotropic gold nanoparticles using cinnamon with superior antibacterial activity, Mat. Res. Express, vol. 6(7), pp. 075043.
[15] Irfan, M., Moniruzzaman, M., Ahmad, T., Mandal, P. C., Abdullah, B., & Bhattacharjee, S. (2017). Growth kinetic study of ionic liquid mediated synthesis of gold nanoparticles using *Elaeis guineensis* (oil palm) kernels extract under microwave irradiation, Arab. J. Chem., pp. 1-12.
[16] Hoshyar, R., Khayati, G. R., Poorgholami, M., & Kaykhaii, M. (2016). A novel green one-step synthesis of gold nanoparticles using crocin and their anti-cancer activities, J. Photochem. Photobiol. B: Biol., vol. 159, pp. 237-242.
[17] Barrios-Gumiel, A., Sánchez-Nieves, J., Pedziwiatr-Werbicka, E., Abashkin, V., Shcharbina, N., Shcharbin, D., & Bryszewska, M. (2019). Effect of PEGylation on the biological properties of cationic carbosilane dendronized gold nanoparticles, Internat. J. Pharm., pp. 118867.
[18] Jasmine, F., Shazia, M., Ali, S. M., Masihur, R., & Huma, M. (2016). Phyto-Chemical Analysis, In-Vitro Antioxidant Potential and GC-MS of *Lallemantia royleana* seeds. International Journal of Scientific and Research Publications, 6(2), 407-411.
[19] Patra, J. K., Kwon, Y., & Baek, K. H. (2016). Green biosynthesis of gold nanoparticles by onion peel extract: synthesis, characterization and biological activities, Advan. Powder Tech., vol. 27(5), pp. 2204-2213.
[20] Amin, M., Iram, F., Iqbal, M. S., Saeed, M. Z., Raza, M., & Alam, S. (2013). Arabinoxylan-mediated synthesis of gold and silver nanoparticles having exceptional high stability, Carb., Poly., vol. 92(2), pp. 1896-1900.
[21] Rajan, A., Vilas, V., & Philip, D. (2015). Studies on catalytic, antioxidant, antibacterial and anticancer activities of biogenic gold nanoparticles, J. Mol. Liquids, vol. 212, pp. 331-339.
[22] Sathishkumar, G., Jha, P. K., Vignesh, V., Rajkuberan, C., Jeyaraj, M., Selvakumar, M., Jha, R., & Sivaramakrishnan, S. (2016). Cannonball fruit (*Couroupita guianensis, Aubl.*) extract mediated synthesis of gold nanoparticles and evaluation of its antioxidant activity, J. Mol. Liquids, vol. 215, pp. 229-236.